[4]A more detailed and comprehensive account of the exact numerical work will be published elsewhere. Here estimates are made with the data available from A. A. Abrikosov, Zh. Eksperim. i. Teor. Fiz. 47, 720 (1964) [translation: Soviet Phys.-JETP 20, 480 (1965)]; and H. J. Fink, Phys. Rev. Letters 14, 309 (1965).

[5]Fink, reference 4.

SURFACE THERMAL DIFFUSE SCATTERING FROM TUNGSTEN*

Judith Aldag† and R. M. Stern

Polytechnic Institute of Brooklyn, Brooklyn, New York

(Received 15 March 1965)

We have observed an anisotropic diffuse background superimposed on the expected low-energy electron diffraction pattern from the clean (110) surface of a tungsten single crystal, using a Varian system, with 230- to 700-eV electrons over the temperature range from 300 to 1600°K. No such structured background appears in the x-ray diffraction patterns from tungsten.[1]

We attribute this anisotropic background to thermal diffuse scattering from a region near the surface of the tungsten crystal.

It has been found by Wallis and others[2-6] that the introduction of a surface to an infinite elastic continuum and to a one-dimensional chain crystal introduces surface normal modes in addition to the bulk modes. The solution for a three-dimensional crystal with surface does not exist. These modes must be considered in the interpretation of the diffraction pattern because the low penetration of low-energy electrons requires the major part of the scattering to take place near the surface, where these modes are important. Surface modes are described by amplitudes (u_{nqj}) which decay exponentially with increasing distance from the surface into the crystal.

It is assumed that the deviation of the ionic position from equilibrium ($\vec{u}_n$) can be described by a superposition of the normal modes of vibration of the crystal[7-10]:

$$\vec{u}_n = \sum_{qj} u_{nqj} \vec{e}_{qj} \exp(i\omega_{qj} t + 2\pi i \vec{q}\cdot\vec{r}_n),$$

where $\vec{e}_{qj}$ is the polarization vector of the phonon of wave vector $\vec{q}$ and polarization j; ω_{qj} is the angular frequency of the phonon; and $\vec{r}_n$ is the vector position of the nth atom in the undisplaced crystal.

As a first approximation, the exponential decay of the surface mode amplitudes will be neglected, and we will use instead a model in which the amplitude is represented by a step function. The scattered intensity from the vibrating crystal is then due to the entire phonon spectrum, including the surface modes. We assume that the electron scattering takes place in this region where the surface modes have nonzero amplitude, which we define as the surface layer.

The intensity function can therefore be written as[10,8]

$$I(\vec{S}/\lambda) = |f_0|^2 e^{-2M} \sum_N I_N$$

$$= |f_0|^2 e^{-2M} (I_0 + I_1 + \cdots I_N),$$

where

$$I_0(\vec{S}/\lambda) = \sum_{nn'} \alpha_n \alpha_{n'} \exp[2\pi i (\vec{S}/\lambda)\cdot(\vec{r}_n - \vec{r}_{n'})]$$

is the Bragg scattering function of the undisplaced lattice,

$$I_1(\vec{S}/\lambda) = \tfrac{1}{2} \sum_{qj} G_{qj} [I_0(\vec{S}/\lambda + \vec{q}) + I_0(\vec{S}/\lambda - \vec{q})]$$

is the thermal diffuse scattering intensity function due to single-phonon processes, and $I_N(\vec{S}/\lambda)$ is the Nth-order phonon-process intensity function.

$$G_{qj} = [\hbar/(2mn)][(k\vec{S}\cdot\vec{e}_{qj})^2/\omega_{qj}] \coth(\hbar\omega_{qj}/2kT)$$

is the amplitude of the intensity I_1 of the scattering due to the single phonon qj, and $\vec{S}/\lambda = \vec{k} - \vec{k}'$ is the scattering vector of the electron (see Fig. 1). Here α_n is an attenuation factor describing the decrease in scattering as the electron beam penetrates the crystal.[11] $\exp(-2M)$ is the Debye-Waller factor.

Since I_0 has appreciable values only when its argument is a vector in the reciprocal lattice, we see that the value of I_1 at $\vec{S}/\lambda$ is due to the contribution of the single phonon q which satis-

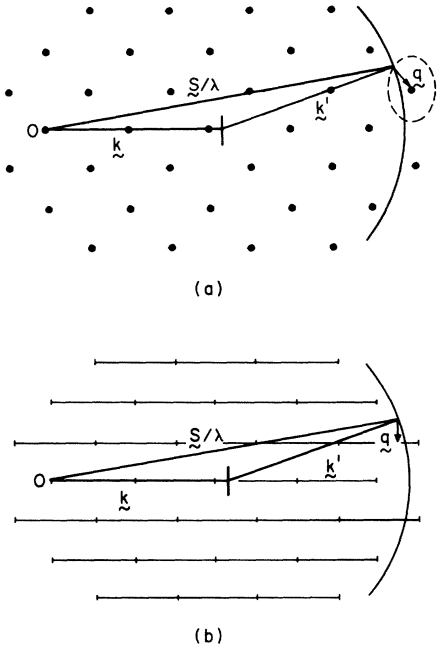

FIG. 1. The vector diagram for single-phonon scattering of an electron by a lattice phonon for (a) a three-dimensional lattice, and (b) a two-dimensional lattice, where $\vec{S}/\lambda$ is the diffraction vector and $\vec{q}$ is the phonon wave vector, to the nearest reciprocal lattice point (a), or rod (b).

fies the requirement $\vec{S}/\lambda \pm \vec{q} = \vec{g}$ (as shown in Fig. 1). The statement that the maximum of I_1 occurs when $\vec{S}/\lambda \pm \vec{q} = \vec{g}$ is equivalent to the statement of conservation of momentum for the single-phonon scattering of the electron ($\vec{k} = \vec{k}' \pm \vec{q} = \vec{g}$) (conservation of energy: $\hbar\omega_k - \hbar\omega_{k'} \pm \hbar\omega_q = 0$). To each phonon $\vec{q}$ there will correspond two maxima in the spatial scattering distribution, of magnitude ($\frac{1}{2}e^{-2M}G_{qj}$), each of which will have the same form as the main maximum but will be symmetrically disposed on either side of it at vector distance $\pm\vec{q}$.

The temperature dependence of I_1 is contained in G_{qj}, and leads to increasing I_1 with increasing temperature. The temperature dependence of the total diffuse background is then due to a combination of the Debye-Waller factor and the temperature dependence of G_{qj}.

The reciprocal lattice of a crystal undergoing normal vibrations consists of the normal (hkl) diffraction points each surrounded by a diffuse region[12] (see Fig. 1). The anisotropy in the diffuse diffraction is directly related to anisotropies in the phonon dispersion curve, as seen in the proportionality of G_{qj} to ω_{qj}.

This diffuse background increases with increasing order of the associated diffraction maxima, since G_{qj} is directly related to the square of S: $[S^2 = (h^2+k^2+l^2)a^2]$. We should therefore expect the thermal diffuse scattering to be more intense for higher order scattering.

Figure 2 shows Lonsdale's[10] calculated thermal diffuse intensity function for the (110) reciprocal net in sodium. The diagram illustrates the type of background to be expected for anisotropic thermal diffuse scattering.

Figure 3(a) is a photograph of the low-energy electron diffraction pattern from a (110) tungsten crystal at 609 eV. The similarities in the streaks and wings associated with diffraction spots with those shown in Fig. 2 should be noted.

The wings and streaks appear in symmetry directions which are expected to be pure mode directions in the bulk. However, no analytic solutions of the equations of elasticity theory exist for the normal modes of an elastic crystal with free anisotropic surfaces, and we speculate that the pure mode directions in the surface are the symmetry directions.

At voltages below approximately 230 V the structured background is not distinguishable to the eye because the orders of the permitted diffractions are too low for $G_{qj} \sim (h^2+k^2+l^2)$ to have appreciable magnitude. The measured intensity of the thermal diffuse scattering closely follows the expected square-law dependence on order.[13] As the voltage is continuously varied the radius of the Ewald sphere changes

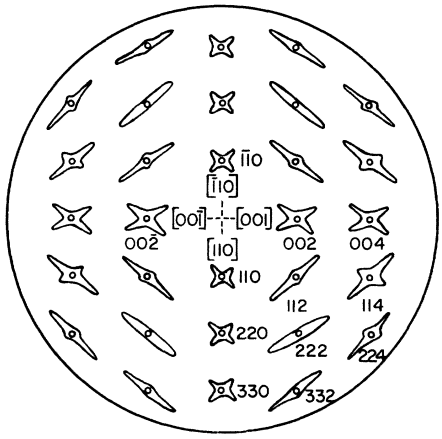

FIG. 2. The intensity distribution, I_1, in a reciprocal lattice plane normal to the [110] direction for sodium (as calculated by Lonsdale[10]).

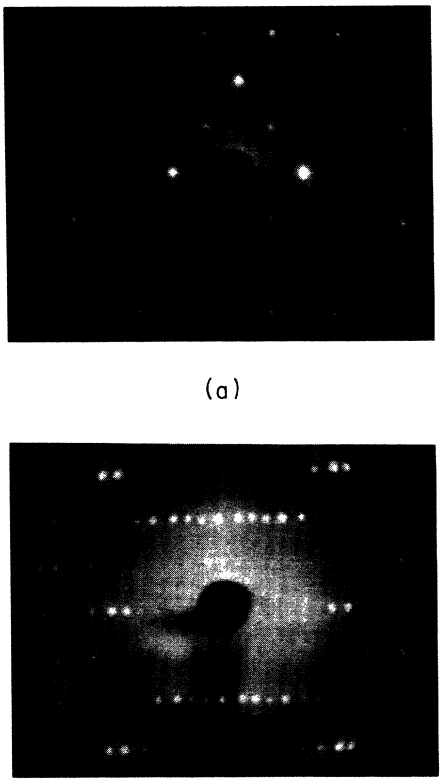

FIG. 3. (a) The diffraction pattern from the (110) surface of tungsten at 609 eV showing the thermal diffuse background. The vertical axis is [001]. The horizontal axis is the [110]. (b) Multiple exposure of the diffraction pattern for rotation of the crystal in 2° steps.

continuously, thus intersecting different sections of reciprocal space. The diffuse background changes continuously, corresponding to the changes of the intersection of the Ewald sphere with an extended diffuse reciprocal lattice.

When the crystal is rotated (equivalent to a rotation of the Ewald sphere through the reciprocal space) the diffuse background rotates with the diffraction maxima but suffers a continuous displacement with respect to its associated maximum, again as expected for an extended reciprocal lattice.

The electrons contributing to thermal anisotropic diffuse scattering have undergone inelastic scattering losses of about 0.1 eV (i.e., corresponding to creation or destruction of a lattice phonon). The diffraction pattern contains electrons which have lost up to 7 eV. We therefore cannot determine the extent to which the electrons contributing to the background are inelastic. It is found that the total secondary current increases monotonically with increasing energy loss at all incident energies above 40-eV primary voltage, indicating that the secondary electrons are scattered with no characteristic energy loss.

Observed structured background has been explained by Kikuchi line scattering.[14] We have eliminated this possibility to our satisfaction.[13]

The dark ring which appears at approximately 45° is associated with the atomic scattering factor. Figure 3(b) is a multiple exposure taken as the crystal was rotated in 2° steps. Since the dark region remains fixed with respect to the incident beam, it must be a characteristic of the atomic scattering factor rather than a crystallographic diffraction phenomenon. This has been discussed by Lander and Morrison.[15] The fact that an atomic scattering phenomenon appears so strongly supports the use of the atomic scattering factor f_0 for each atom of the crystal modified by the factor α_n which describes the attenuation in the scattering from the atoms below the surface.

Figure 4 shows the intensity of the (−3.1) diffraction spot at 690 V ($h = 8$, $k = 11$, $l = 1$) measured with a Spectra Pritchard photometer with an angular aperture of 15′ as a function of heating current and approximate crystal tem-

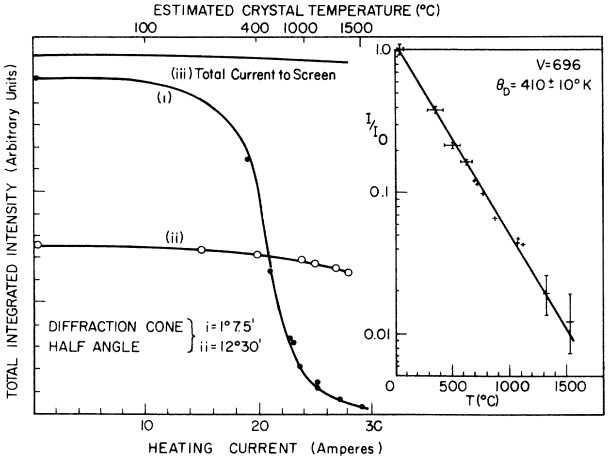

FIG. 4. Intensity versus temperature for (i) the (−3.1) diffraction spot at 690 V measured with photometer aperture of 15′, (ii) the spot plus its background, measured with photometer aperture of 2°, and (iii) the total electron current to the screen. The inset shows log$I$ vs T yielding an effective Debye temperature of 410°K.

perature. The second curve represents the intensity of the spot plus its background measured with an aperture of 2°. The third curve shows the total current to the screen. These curves are not normalized to the same scale. The total current scattering into the region is maintained at a constant value while the scattering into the Bragg maxima decreases as expected from the Debye-Waller effect.[11,16-18] The inset shows $\log I$ vs T yielding an effective Debye temperature of 410°K.[19] It is also observed that the background remains structured to at least 1500°K. This leads us to believe that the loss of energy in the Bragg reflection is at least partially compensated for by the increases in the coherent thermal diffuse scattering. This is in accordance with the predicted increase in intensity of I_1.

We conclude that the observations are of thermal diffuse scattering, from anisotropic surface modes. Bulk diffuse scattering, as in the x-ray diffraction, is weak and isotropic due to the bulk isotropy of tungsten. Surface thermal diffuse scattering should be of use in investigating dispersion relationships for surface phonons.

X rays and slow neutrons[20-22] have been used to investigate the phonon spectrum in bulk. In the investigation of the spectrum by slow neutrons the dispersion curves are obtained directly from conservation of energy and momentum. The energy change due to absorption or emission of a typical phonon is of the same order of magnitude as the energy of the neutron, and is easily detected. In x-ray diffraction the energy of the x rays is so large compared to that of the phonons that the energy loss is insignificant. However, the intensity of the radiation is proportional to the thermal excitation of the mode, and to the frequency. By looking along symmetry axes where the polarization directions are known, the dispersion relations (at least for these special directions) can be obtained. In low-energy electron diffraction investigations, in addition to the difficulty in separating bulk and surface modes and their states of polarization, there are unresolved questions, now being considered, in the derivation of the intensity when attenuated surface modes are involved. These questions must be settled before dispersion relations for surface modes can be obtained.

---

*Work supported by the U. S. Air Force Contract No. AF49(638)1369.

†National Science Foundation Cooperative Graduate Fellow.

[1]Judith Aldag and R. M. Stern, Bull. Am. Phys. Soc. 10, 69 (1965).

[2]R. F. Wallis, Surface Sci. 2, 155 (1964).

[3]R. F. Wallis, Phys. Rev. 105, 540 (1957).

[4]R. F. Wallis and D. C. Gazis, Phys. Rev. 128, 106 (1960).

[5]D. C. Gazis, R. Herman, and R. E. Wallis, Phys. Rev. 119, 533 (1960).

[6]M. Ashkin, Phys. Rev. 136, A821 (1964).

[7]Max Born and Kun Huang, Dynamical Theory of Crystal Lattices (Clarendon Press, Oxford, England, 1954).

[8]A. A. Maradudin, E. W. Montroll, and G. H. Weiss, Solid State Physics, Supplement No. 3 (Academic Press, Inc., New York, 1963), Chaps. II, III, and VII.

[9]J. M. Ziman, Electrons and Phonons (Clarendon Press, Oxford, England, 1960), Chaps. I, II, and V.

[10]R. W. James, Optical Principles of Diffraction of X Rays (G. Bell and Sons, Ltd., London, 1962), Chap. V.

[11]A. U. MacRae, Surface Sci. 2, 522 (1964).

[12]The diffuse region is the plot in reciprocal space of the intensity function I_1.

[13]To be published in detail.

[14]E. G. McRae and C. W. Caldwell, Jr., Surface Sci. 2, 509 (1964).

[15]J. J. Lander and J. Morrison, J. Appl. Phys. 34, 3517 (1963).

[16]A. U. McRae and L. Germer, Phys. Rev. Letters 8, 489 (1962).

[17]A. A. Maradudin and J. Melngailis, Phys. Rev. 133, A1188 (1964).

[18]A. A. Maradudin and P. A. Flinn, Phys. Rev. 129, 2529 (1963).

[19]The effective Debye Θ is found to decrease continuously with decreasing voltage. At 72 V for the (440) spot at near normal incidence, $\Theta = 245°$.[13]

[20]R. J. Birgeneau, J. Cordes, G. Dolling, and A. D. B. Woods, Phys. Rev. 136, 1112 (1962).

[21]A. D. B. Woods, B. N. Brockhouse, R. H. Marsh, and A. T. Steward, Phys. Rev. 128, 1112 (1962).

[22]B. N. Brockhouse, T. Arase, G. Caglioti, K. R. Rao, and A. D. B. Woods, Phys. Rev. 128, 1099 (1962).

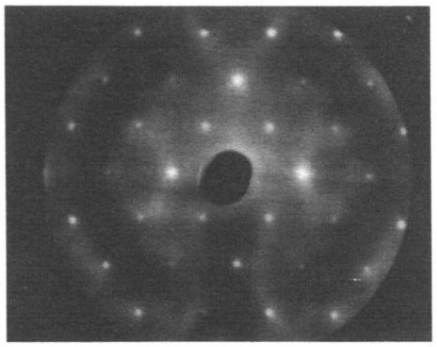

(a)

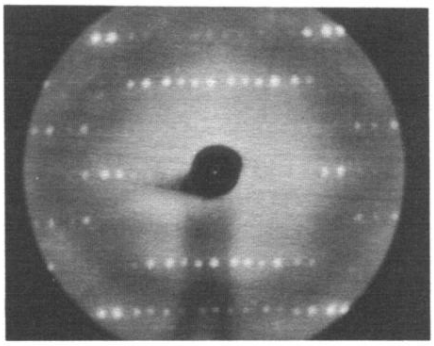

(b)

FIG. 3. (a) The diffraction pattern from the (110) surface of tungsten at 609 eV showing the thermal diffuse background. The vertical axis is [001]. The horizontal axis is the [110]. (b) Multiple exposure of the diffraction pattern for rotation of the crystal in 2° steps.